Fish and Shellfish Immunology 93 (2019) 517–530

Contents lists available at ScienceDirect

Fish and Shellfish Immunology

journal homepage: www.elsevier.com/locate/fsi

Full length article

The effect of rearing density on immune responses of hepatopancreas and intestine in *Litopenaeus vananmei* against *Vibrio paraheamolyticus* E1 challenge

Yilong Wang[a,b,c], Baojie Wang[a,b], Xuqing Shao[f], Jianchun Shao[a,b,c], Mei Liu[a,b], Mengqiang Wang[a,b,d,**], Lei Wang[a,b,e,*]

[a] CAS Key Laboratory of Experimental Marine Biology, Institute of Oceanology, Chinese Academy of Sciences, Qingdao, 266071, China
[b] Laboratory for Marine Biology and Biotechnology, Qingdao National Laboratory for Marine Science and Technology, Qingdao, 266237, China
[c] University of Chinese Academy of Sciences, Beijing, 100049, China
[d] Research Platform for Marine Molecular Biotechnology, National Laboratory for Marine Science and Technology, Qingdao, 266237, China
[e] CAS Center for Ocean Mega-Science, Chinese Academy of Sciences, Qingdao, 266400, China
[f] Shandong Cigna Detection Technology Co., Ltd, Qingdao, 266237, China

ARTICLE INFO

Keywords:
Rearing density
Vibrio parahaemolyticus E1
Transcriptome
Histopathology
Antioxidant status

ABSTRACT

Rearing density and disease management are considered as pivotal factors determining shrimp farm productivity and profitability. To systematically investigate the potential mechanisms for density-related differences between disease susceptibility and rearing densities, we conducted comparative transcriptome analysis of the molecular differences between hepatopancreas and intestine of *Litopenaeus vannamei* under two different rearing densities (800- and 400- shrimp/m^3) for 15 d and further analyzed the differences in immune response to *Vibrio parahaemolyticus* E1 (VPE1) raised under two density conditions. Totally 45 different expression genes (DEGs) were identified in the hepatopancreas under two different rearing densities, the DEGs were grouped into four processes or pathways related to animal immune system. Then, exposure to the VPE1 resulted in 639 DEGs, involved into fourteen immune related processes or pathways. In the intestine, seventeen processes or pathways related to the immune system were identified among the 5470 DEGs under two different rearing densities. 279 DEGs were identified post VPE1 challenge, classified into five processes or pathways associated with the immune system. Meanwhile, the results of growth performance, histopathology and the activities of antioxidant enzymes in the hepatopancreas and intestines of shrimp showed that high density decreased weight gain rate (63.20 ± 1.67% and 18.73 ± 3.35% in the high and low rearing density groups, respectively), severely destroyed the histopathology and inhibited the antioxidant enzymes activities. This study demonstrated that rearing density in *L. vannamei* significantly impacts susceptibility to the VPE1, via altered transcriptional challenge responses, and thus higher mortality due to disease.

1. Introduction

Litopenaeus vannamei is one of the most commonly cultured shrimp species widely distributed in the world [1]. With the aim of increasing profitability, intensive farming mode, based on the utilization of high rearing density (HD) and artificially formulated feed to achieve continuous increase in their production, is employed in aquaculture practice and becoming prevalent [2,3]. Nevertheless, persistent HD culture could exert adverse effects on shrimp growth, immune function, reproduction and increase disease susceptibility [4,5]. Therefore, studying the underlying biological mechanisms caused by rearing density stress and mitigating its negative effects through corresponding aquaculture practices will help improve animal welfare and productivity. Studies on rearing densities have been conducted in many shrimp species, such as *L. vannamei* [6], *Fenneropenaeus chinensis* [7], *Penaeus monodon* [8], *Lysmata seticaudata* [9], *Palaemonetes varians* [10], and *Penaeus esculentus* [11]. These studies mainly focused on growth performance, antioxidant enzymes, and the expression of certain genes. But, how such stress impact transcriptional responses to pathogen challenge is still limited and systematic and in-depth research

* Corresponding author. Institute of Oceanology, Chinese Academy of Sciences, 7 Nanhai Road, Qingdao, 266071, China.
** Corresponding author. Institute of Oceanology, Chinese Academy of Sciences, 7 Nanhai Road, Qingdao, 266071, China.
E-mail addresses: wangmengqiang@qdio.ac.cn (M. Wang), leiwang@qdio.ac.cn (L. Wang).

https://doi.org/10.1016/j.fsi.2019.08.004
Received 6 June 2019; Received in revised form 27 July 2019; Accepted 2 August 2019
Available online 03 August 2019
1050-4648/

is needed.

For the past few years, stress, pathogens, and parasites were the most devastating and virulent agents threatening aquaculture culture industry, causing substantial economic losses [12–15]. It is unclear whether the challenge level and mortality of shrimp against pathogens are related to increased pathogen susceptibility or decreased immune response capacity caused by environmental stress. Thus, to understand the stress of rearing density on the immune response of shrimp and their resistance to pathogens is pre-requisite. *Vibrio parahaemolyticus*, as one of the most hazardous pathogens in shrimp aquaculture, could induce acute hepatopancreatic necrosis syndrome (AHPNS) or early mortality syndrome (EMS), which have been responsible for widespread mortality of farmed white shrimp in South East Asia [16,17]. Although several previous studies have analyzed such responses to a combination of high density and pathogen challenge. For example, Lin et al. reported exposure to extreme high densities (10–40 shrimp/L) during up to 12 h decrease resistance to *Vibrio alginolyticus* and white-spot syndrome virus (WSSV) mainly by a depressed immune capacity [4]. Liu et al. reported that the immune status and welfare of white shrimp can be seriously impaired in the high rearing density condition (500 shrimp/m^3) in biofloc systems [18]. Still, the biological mechanism between stress of rearing density and the shrimp susceptibility to pathogen, especially *V. parahaemolyticus*, were rarely reported.

The hepatopancreas and intestine, playing an important role in immune defense, digestive, nutrient absorption and metabolism, are the two most critical organs in marine invertebrates [19,20]. The healthy hepatopancreas and intestine are critical for the growth, metabolism and immunity of hosts. However, the hepatopancreas and intestine of hosts are vulnerable to environmental stress and pathogens, resulting in the dysfunction of hosts physiochemical activities, and lead to diseases and death [4,21]. Therefore, the relationship between environmental stress and disease susceptibility can be through analyzing potential morphological, biochemical, and microarray changes in the hepatopancreas and intestine of host in response to pathogen challenge between different rearing densities.

In this study, to systematically investigate the potential mechanisms for density-related differences between disease susceptibility and rearing densities, we conducted comparative transcriptome analysis of the hepatopancreas and intestine of *L. vannamei* under two different rearing densities (800- and 400- shrimp/m^3) for 15 d and further analyzed the differences in immune response to *V. parahaemolyticus* E1 (VPE1) raised under two density conditions. Meanwhile, we determined growth performance, histopathology and the activities of several important antioxidant enzymes in the intestines and hepatopancreas. The results of this study not only provide a significant in-depth transcriptomic resource for future studies of rearing stress and immunity in shrimp, but offer a foundation for finding potential and feasible practical strategies for health management and disease prevention in shrimp aquaculture.

2. Materials and methods

2.1. Shrimp rearing conditions

Before the start of the feeding trial, apparently healthy *L. vannamei* obtained from a commercial shrimp farm Ruizi Seafood Development Co. Ltd. (Qingdao, China) were acclimatized for a week before the experiments, at 28 ± 2 °C in oxygenated seawater (30–31‰ salinity). In the study, we conducted two rearing densities according to the shrimp culture practice under field conditions. The common tank size is generally about 670 m^2 in shrimp farms, rearing amounts ranges from 300,000 to 500,000 shrimps/tank, stands for 500 to 833 shrimps/m^3. Additionally, some previously reported studies on the effect of rearing density on the growth and immunity of *L. vannamei* also mainly refer to this standard [18,22,23]. So, the shrimp were classified into two groups according to our practice rearing conditions: 400 shrimp/m^3 as the low density (LD), 800 shrimp/m^3 as the high density (HD). Each group had three replicates. Then, shrimp of similar sizes (initial mean weight, 7.52 ± 0.12 g) were randomly distributed into 6 1000-L cylindrical tanks contained 750 L seawater for 15 d. Shrimp was hand-fed three times daily at 07:00 a.m., 12:00 a.m., and 6:00 p.m. with a commercial shrimp feed purchased from Yantai Dale Feed Co. Ltd (Shandong, China) for 15 consecutive days. During this experimental period, basic zootechnical variables (growth, survival and water quality) were recorded. To avoid the effect of water quality on the experimental results, the water temperature was controlled at 29–31 °C; pH, 8.4–8.6; dissolved oxygen, 5.5–6.3 mg/L; ammonia nitrogen, less than 0.1 mg/L; and nitrite nitrogen, less than 0.1 mg/L. The samples collection and analysis were done as specified below.

2.2. Preparation and challenge of VPE1

The VPE1 strain was donated by Dr. Zhaolan Mo from Yellow Sea Fisheries Research Institute Chinese Academy of Fishery Sciences. The pathogenic strain VPE1 was cultured in 2216E broth and incubated in a shaking (150 rpm) incubator at 28 °C for 20 h before challenge. 240 shrimps from LD group and 240 shrimps from HD group were randomly divided into three 400-L cylindrical tanks (each containing 300 L seawater), respectively, including two groups: LD challenge group (LDC) and HD challenge group (HDC). Each group had three replicates with 80 shrimp per replicate. Through preliminary test, we determined the lowest VPE1 challenge dose (1×10^{-8} cfu/mL of the final concentration) required to achieve about 50% mortality by infiltration challenge at 72 h post challenge (Fig. S1). Therefore, a final concentration of 1×10^{-8} cfu/mL VPE1 were chosen for experimental challenge. During the 72 h VPE1 challenge experimental period, growth and survival of shrimp were recorded every 12 h and removing dead shrimp in time. The samples collection and analysis were done as specified below.

2.3. Sample collection

The experiments encompassed two densities groups (LD and HD groups) for 15 d and two density-challenge groups (LDC and HDC groups) for 72 h with five challenge times (12-, 24-, 48-, 60- and 72- h). Hepatopancreas and intestine tissue samples in live shrimp were collected at 15 d from LD and HD groups, and 12-, 24-, 48-, 60- and 72- h from LDC and HDC groups, respectively. Each group included three replicates with 8 shrimp hepatopancreas and intestine tissue samples per replicate. The hepatopancreas and intestine tissue samples were examined at 15 d (after rearing at LD and HD conditions) and 48 h (after VPE1 challenge) in the following transcriptome and histopathology analysis experiments. The 15 d and 48 h time points were chosen based on pre-experiments that showed mostly significant expression of immune-related genes and the highest mortality after VPE1 challenge at the two time points (Fig. S2 and Fig. S3).

2.4. Histopathology

After feeding trials of 15 d and VPE1 challenge of 48 h, the hepatopancreas and intestine tissue of shrimp from LD, HD, LDC, and HDC groups (including 6 live shrimp per group, equal to 2 shrimp per replicate) were obtained and fixed in 10% formalin for 24 h, dehydrated in an ascending alcohol series (50%–95%). Dehydrated tissues were embedded in paraffin, and sectioned into 4 μm thick with a microtome. The 4 μm thick tissues sections were stained with hematoxylin and eosin (H&E), then examined using an ECHO microscope (California, America).

2.5. RNA extraction and sequencing

Total RNA from each sample was extracted using TRIzol reagent (Invitrogen, Carlsbad, CA, USA) according to manufacturer's

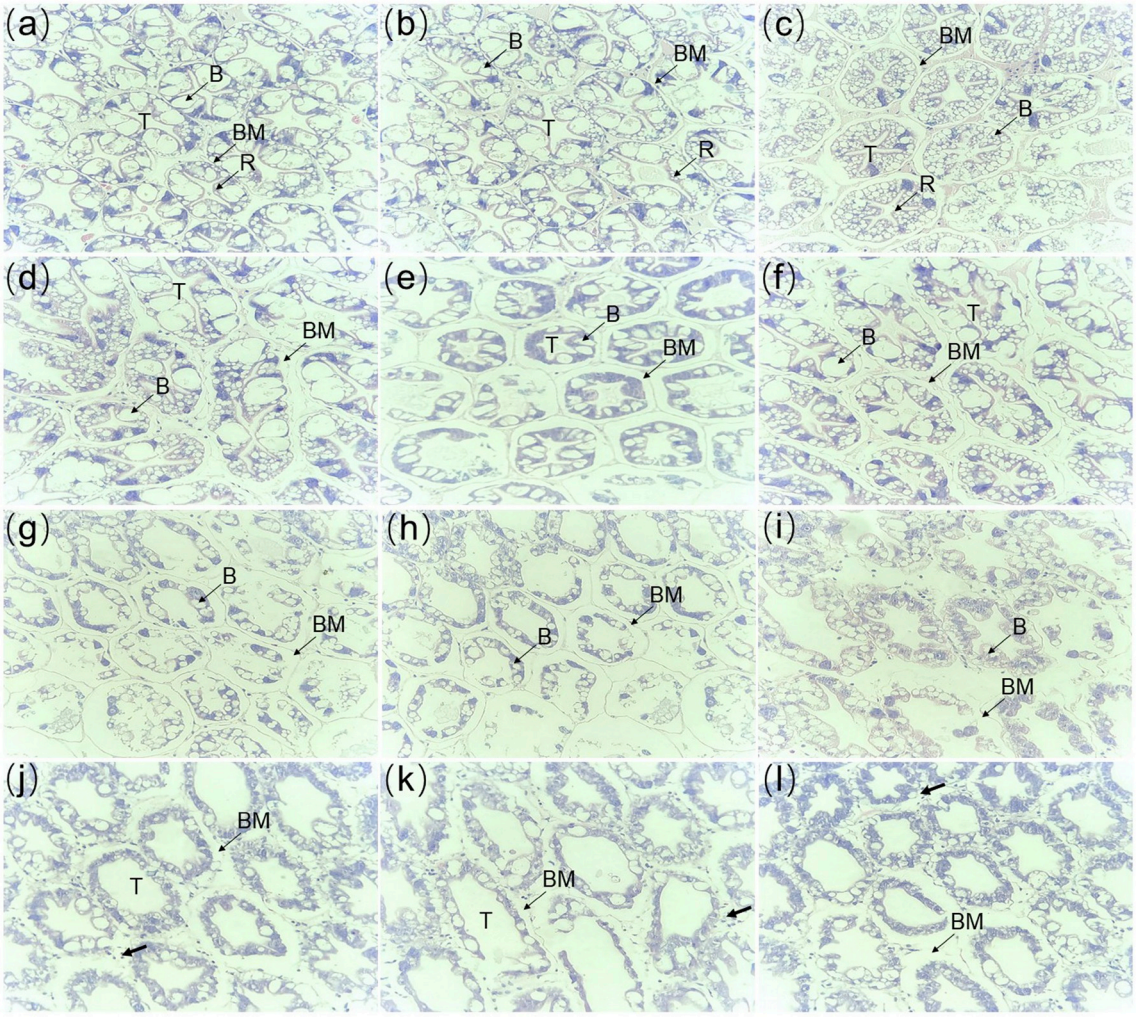

Fig. 1. Effects of stocking density and VPE1 infection on histomorphology of hepatopancreas of *L. vannamei*. a–c: the hepatopancreas tissues from LD group; d–f: the hepatopancreas tissues from HD group; g–i: the hepatopancreas tissues from LDC group; j–l: the hepatopancreas tissues from HDC group; B: secretory cells (B-cell); R: storage cells (R-cell); The bold arrow: hemocytes; BM: basement membrane; T: star-shaped polygonal structures of the lumen of hepatopancreas. Stained with hematoxylin and eosin (H & E), 200 × .

instructions. Then mRNA was enriched by removing rRNA by Ribo-Zero™ Magnetic Kit (Epicentre), fragmented into short fragments using fragmentation buffer and reverse transcripted into cDNA with random primers. Second-strand cDNA was synthesized with RNase H, DNA polymerase I, dNTP and buffer. The cDNA fragments were purified using QiaQuick PCR extraction kit, and the purified fragments were experienced with end repaired, poly(A) added, and ligated to Illumina sequencing adapters. The final ligation products were size selected by using agarose gel electrophoresis, PCR amplified, and sequenced using Illumina HiSeq™ 2500 by Gene Denovo Biotechnology Co. (Guangzhou, China). The raw reads were deposited into the NCBI Sequence Read Archive (SRA) database (Accession Number: PRJNA554509).

2.6. Bioinformatic analyses

Clean reads were obtained by removing adapters or low quality bases (reads with quality score ≤ 20) and ribosome RNA (rRNA) using short reads alignment tool Bowtie2 [24]. Then, the shrimp Illumina sequences were mapped to reference genome (version: GCF_003789085.1 and accession number: ASM378908v1) by TopHat2 [25] (version 2.0.3.12), respectively. Gene abundances of each group were quantified by software RSEM [26]. The method of FPKM (Fragments Per Kilobase of transcript per Million mapped reads) was used to normalize the gene expression level. The reliability and operational stability of experimental results were evaluated by correlation coefficient analysis of samples. The closer the correlation coefficient approaches to 1, the better the repeatability between two samples. Differentially expressed genes (DEGs) were simultaneously analyzed by using negative binomial distribution and generalized linear model (GLM) in edgeR package (http://www.r-project.org/), respectively. The genes with a fold change ≥ 2 and a false discovery rate (FDR) < 0.05 in a comparison were as significant DEGs. All DEGs were mapped to GO terms in the Gene Ontology database (http://www.geneontology.org/). Hypergeometric test (with FDR correction) was carried out to define significantly enriched biological processes, molecular functions, and cellular components of groups of DEGs comparing to the genome background. Pathway enrichment analysis identified significantly enriched pathways in DEGs comparing with the Kyoto Encyclopedia of Genes and Genomes (KEGG) database (http://www.genome.jp/kegg).

2.7. Enzyme activity assay

The activities of total superoxide dismutase (T-SOD), catalase (CAT), glutathione peroxidase (GSH-PX) and the content of malondialdehyde (MDA) in the hepatopancreas and intestine of shrimp were determined at the 15 d (after rearing at LD and HD conditions)

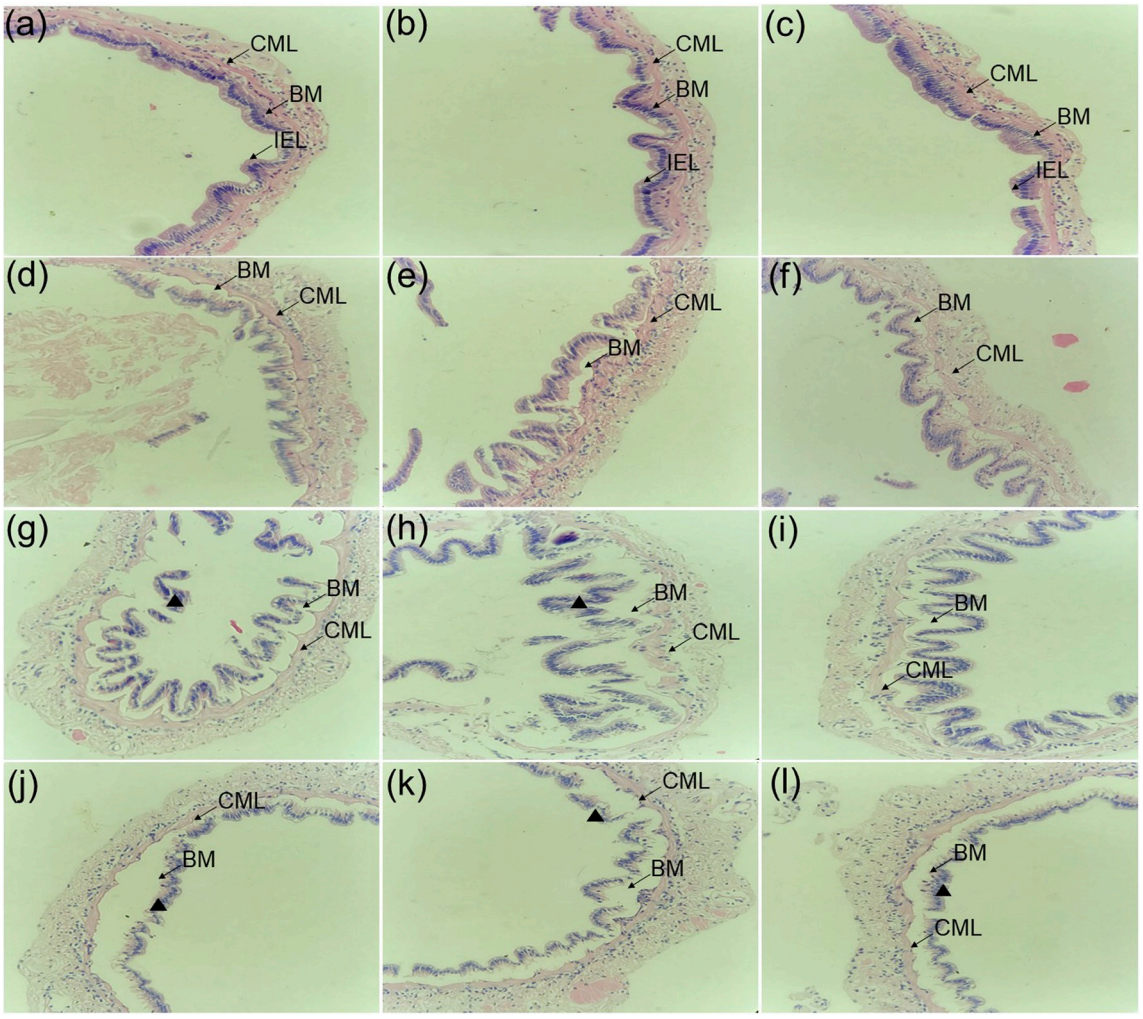

Fig. 2. Effects of stocking density and VPE1 infection on histomorphology of intestine of *L. vannamei*. a–c: the intestine tissues from LD group; d–f: the intestine tissues from HD group; g–i: the intestine tissues from LDC group; j–l: the intestine tissues from HDC group; BM: basement membrane; CML: circular muscle layers; IEL: intestinal epithelial layer; Triangle: exfoliated epithelial tissue of the intestine. Stained with hematoxylin and eosin (H & E), 200 × .

Table 1
Effects of stocking density and VPE1 infection on antioxidant enzyme activities of hepatopancreas and intestine of *L. vannamei*. "*" indicated significant differences between two groups at each treatment ($P < 0.05$).

Parameters	Hepatopancreas				Intestine			
	LD	HD	LDC	HDC	LD	HD	LDC	HDC
CAT (U mg $^{-1}$ protein)	2.56 ± 0.17	1.73 ± 0.36*	5.56 ± 0.91	3.71 ± 0.21*	8.24 ± 0.96	5.84 ± 1.25*	10.41 ± 2.13	5.32 ± 1.37*
T-SOD (U mg $^{-1}$ protein)	29.62 ± 3.14	21.36 ± 2.01*	29.53 ± 2.87	18.61 ± 2.74*	18.38 ± 1.41	15.56 ± 1.98	27.12 ± 1.38	16.53 ± 1.41*
GSH-PX (U mg $^{-1}$ protein)	50.44 ± 2.34	43.17 ± 3.65*	45.91 ± 4.27	36.16 ± 1.79*	24.61 ± 1.37	17.31 ± 1.86*	23.26 ± 1.07	15.76 ± 2.01*
MDA (U mg $^{-1}$ protein)	4.46 ± 0.20	5.42 ± 0.38*	6.79 ± 0.72	8.04 ± 1.27	3.30 ± 0.37	4.41 ± 0.82*	7.12 ± 0.49	7.32 ± 0.84

and 48 h (after VPE1 challenge, respectively) using commercial colorimetric or fluorimetric kits (Nanjing Jiancheng Bioengineering Research Institute).

2.8. The verification of transcriptomic sequencing by quantitative real-time PCR (qPCR)

A total of twenty DEGs were randomly selected in hepatopancreas and intestine for verification and the primers were listed in Table S1 qPCR was performed in a LineGene K Real-Time PCR System (Bioer Technology, Hangzhou, China) to verify the data of transcriptomic sequencing. The expression of genes was calculated as relative expression to beta-actin using the comparative Ct method ($2^{-\triangle\triangle Ct}$ method) [27] and samples were analyzed in triplicates. The thermocycling profile consisted of an initial denaturation at 94 °C for 30 s, followed by 40 cycles at 94 °C for 5 s and 60 °C for 30 s.

2.9. Statistical analysis

The growth parameters were calculated according the following formula: Weight gain (%) = [(Final body weight (g) - Initial body weight (g))/Initial body weight (g)] × 100%. Survival rate (%) = (Final number of shrimps)/(initial number of shrimps) × 100%. Statistical analysis was performed using SPSS software 17.0 (IBM Corp, Armonk, NY, USA). The data is all presented as mean ± standard error (SE) and tested by performing one-way analysis of variance (ANOVA)

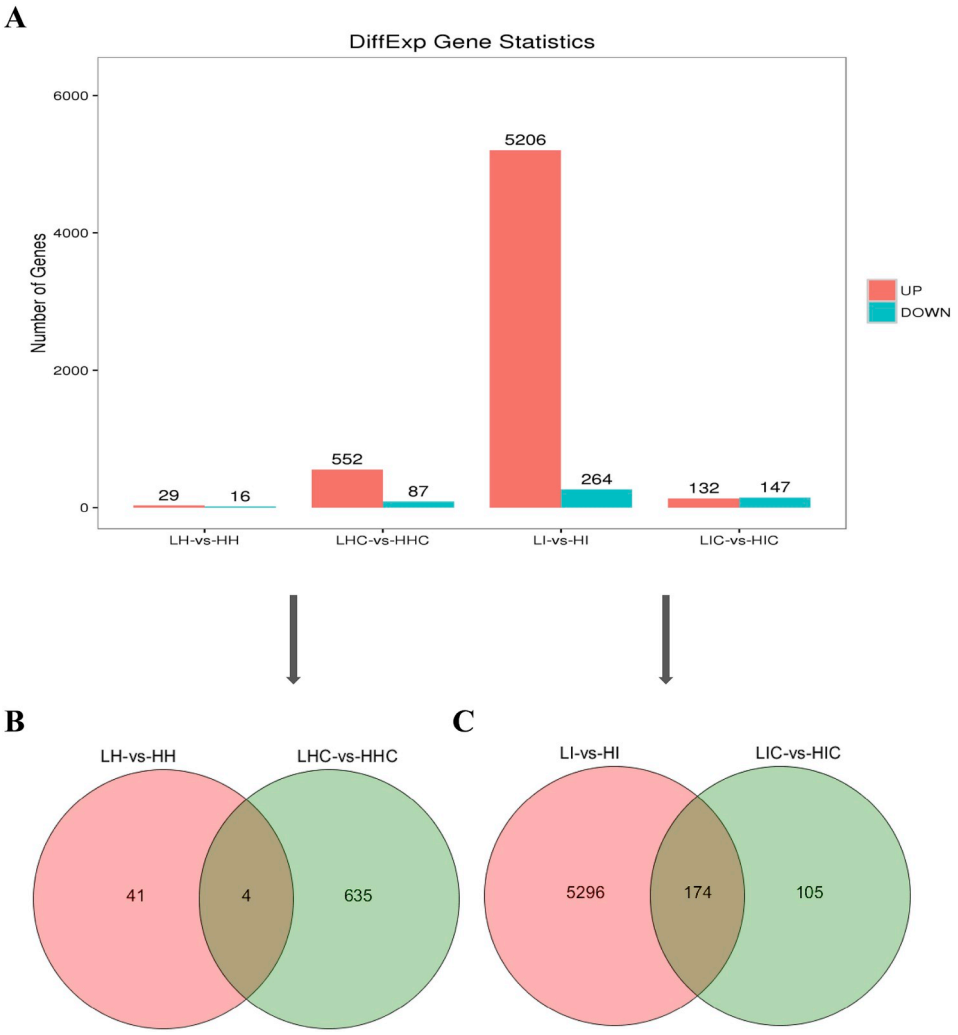

Fig. 3. A. Bar graph of DEGs in hepatopancreas and intestine of *L. vannamei* in each group. **B**. Venn diagram analysis of the number of DEGs in hepatopancreas of *L. vannamei* that are shared or unique between LD-HD and LDC-HDC groups. **C**. Venn diagram analysis of the number of DEGs in intestine of *L. vannamei* that are shared or unique between LD-HD and LDC-HDC groups. DEGs were selected by |fold change| was ≥1 and their q-value was < 0.05.

followed by Dunnett's tests ($P < 0.05$ for significant difference).

3. Results

3.1. Effect of rearing density and VPE1 challenge on shrimp grows and survival

After 15 d of breeding experiments, a significant difference in weight gain ratio of shrimp was observed between the LD (63.20 ± 1.67%) and HD (18.73 ± 3.35%) groups ($P < 0.05$). Then, susceptibility to VPE1 challenge 48 h was studied in shrimp raised under two density conditions. Overall survival rate of shrimp was 77.50 ± 1.62% and 83.75 ± 2.23% in LD and HD VPE1-challenged treatments, respectively.

3.2. Effects of rearing density and VPE1 challenge on histopathology of hepatopancreas and intestine of L. vannamei

Shrimp from HD groups exhibited markedly histological alterations in the hepatopancreas (Fig. 1). There was an obvious separation between the myoepithelial layer and the epithelium, and the columnar epithelial cells of the hepatic ducts became enlarged. Some storage cells (R-cell) and star-shaped polygonal structures of the lumen were blurry and disappeared. Then, exposure to the VPE1 caused further morphology and microstructure of hepatopancreas change in LDC and HDC groups. The columnar cells and star-shaped polygonal structures of the lumen were totally disappeared. Furthermore, compared to the LDC group samples, the hepatopancreas of shrimp in HDC groups showed more severe structural damage. The secretory cells (B-cell) were disappeared and lots of hemocytes infiltrated into the hepatopancreas. Likewise, the microstructure of intestine in HD groups was lesion (Fig. 2). Parts of epithelial cells detached from the basement membrane and destroyed. In most regions of the intestine, especially in HDC groups, epithelial cells completely detached from the basement membrane and destroyed severity after exposure to the VPE1. Epithelial tissue exfoliated and emerged in the bowel lumen.

3.3. Effects of rearing density and VPE1 challenge on antioxidant enzyme activities of hepatopancreas and intestine of L. vannamei

The T-SOD, CAT and GPX activity of hepatopancreas and intestinal were significantly lower in HD and HDC groups than in the LD and LDC groups, respectively. Oppositely, the MDA content of hepatopancreas and intestinal was significantly higher in HD group than in the LD group. In HDC and LDC groups, there was no significant difference in the MDA content of hepatopancreas and intestinal (Table 1).

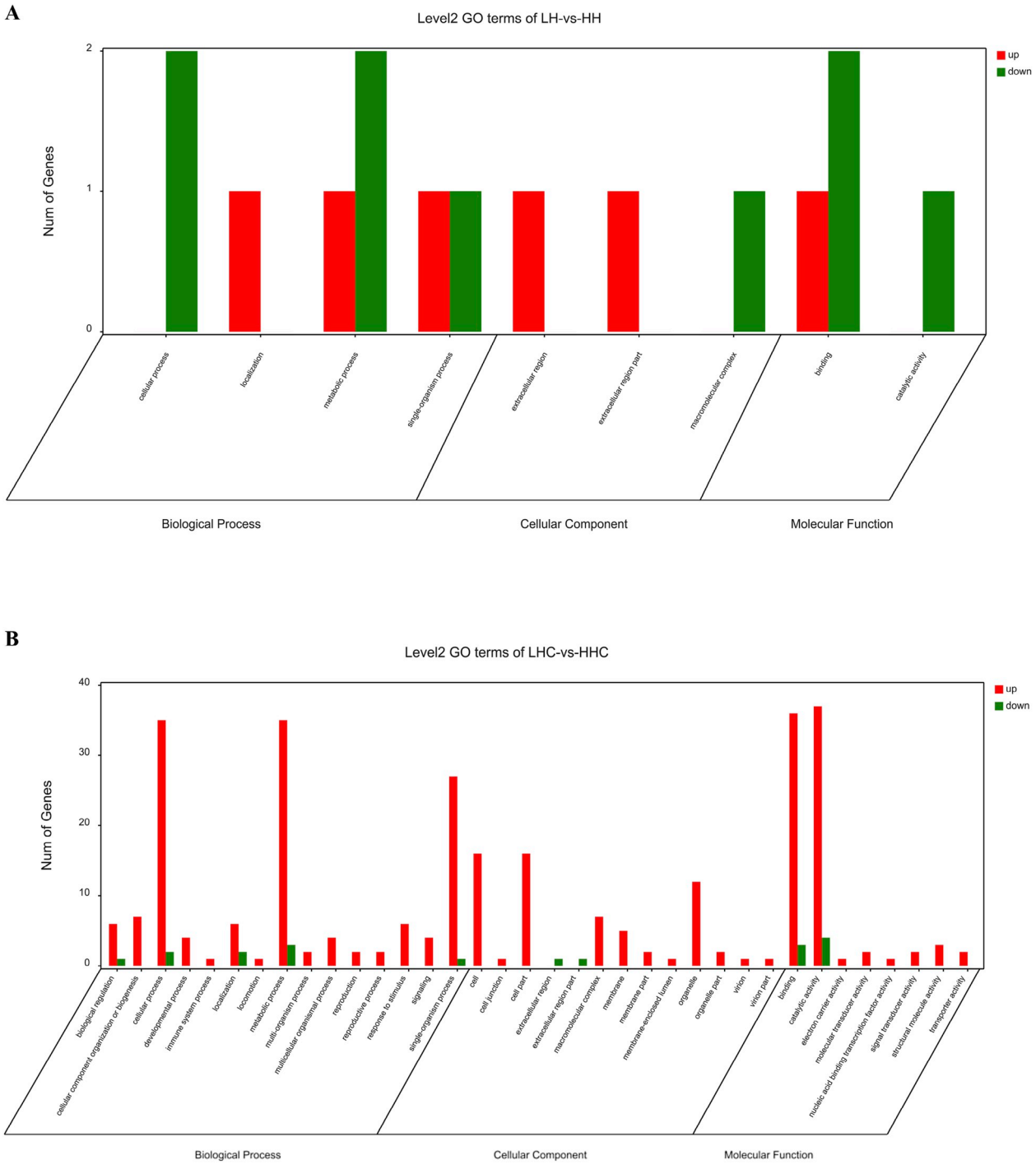

Fig. 4. A. GO enrichment analysis of DEGs in hepatopancreas of *L. vannamei* in LD-HD groups. **B.** GO enrichment analysis of DEGs in hepatopancreas of *L. vannamei* in LDC-HDC groups.

3.4. Transcriptome sequencing

A total of 1,086,767,510 raw sequencing reads were obtained from 24 libraries by using Illumina HiSeq™ 2500. After quality control and removing the reads aligned with ribosomal RNA, 964,618,160 clean reads (88.76%) remained for further analysis. From these clean reads, an average of 75.40% were mapped to the *L. vannamei* genome (Table S2). The gene expression abundance of all samples was mainly concentrated in the range of log10 (FPKM) value −2 to 4 (Fig. S4). Gene expression levels of shrimp in different treatment groups were from high to low, followed by LD group, HD group and VPE1-challenged group, and the gene expression abundance in intestine of shrimp was high than hepatopancreas (Fig. S5). Pearson correlation coefficient between replicates was measured, with an average r coefficient of 0.985, 0.991, 0.958 and 0.939 for LH (hepatopancreas of shrimp from LD group), HH (hepatopancreas of shrimp from HD group), LHC (hepatopancreas of shrimp from LD group after VPE1 challenge) and HHC (hepatopancreas of shrimp from HD group after VPE1 challenge) groups, respectively. The average r coefficient for LI (intestine of shrimp from LD group), HI (intestine of shrimp from HD group), LIC (intestine of shrimp from LD group after VPE1 challenge) and HIC (intestine of shrimp from HD group after VPE1 challenge) groups were

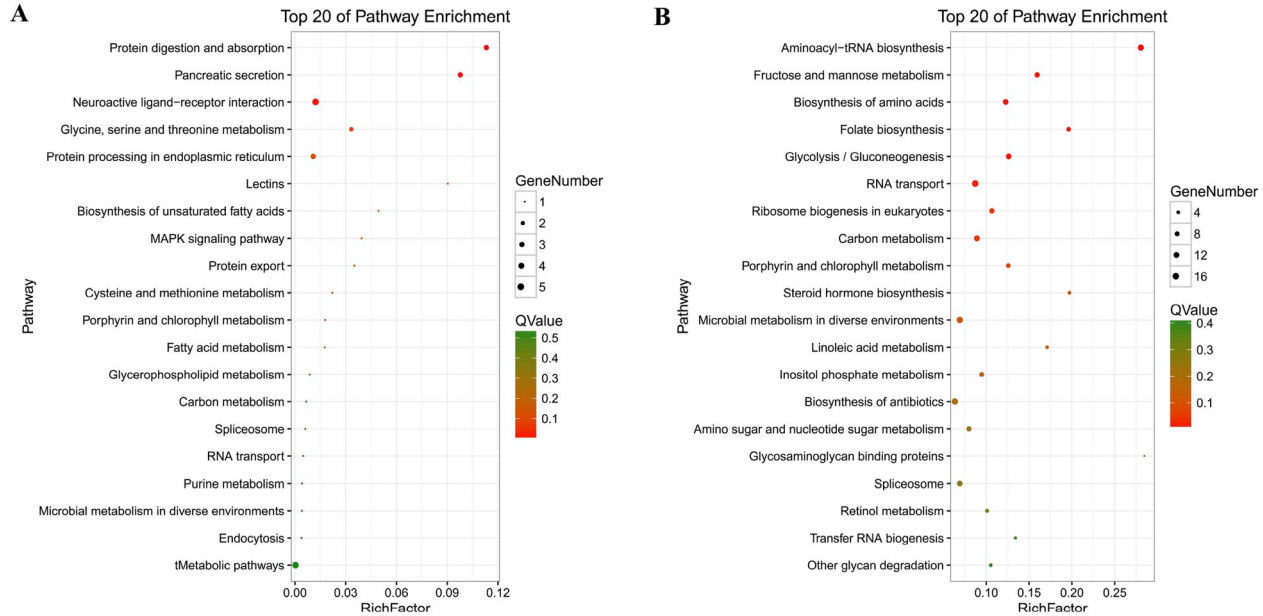

Fig. 5. A. Top 20 significantly enriched KEGG pathways of DEGs in hepatopancreas of *L. vannamei* in LD-HD groups. **B.** Top 20 significantly enriched KEGG pathways of DEGs in hepatopancreas of *L. vannamei* in LDC-HDC groups.

0.976, 0.967, 0.991 and 0.974, respectively (Fig. S6).

3.5. Comparative analysis of the L. vannamei hepatopancreatic transcriptomic response to VPE1 challenge between different rearing densities

In order to investigate the transcriptomic effects of rearing density on *L. vannamei* hepatopancreatic response to VPE1 challenge, we compared gene expression between LH-HH and LHC-HHC groups, respectively. The results of negative binomial distribution difference analysis showed that a total of 45 different expression genes (DEGs) were identified in hepatopancreas from the LH and HH group, with 29 and 16 genes up- and down-regulated, respectively. Then, exposure to the VPE1 resulted in differential expression of 639 genes in LHC and HHC group, corresponding to 552 and 87 genes up- and down-regulated, respectively (Fig. 3A). From all the transcripts that were differently expressed in hepatopancreas of shrimp from LH-HH and LHC-HHC groups, 4 DEGs were shared (Fig. 3B). Only 15 DEGs and 9 terms were enriched by GO enrichment analysis between two rearing densities, involving in metabolic, cellular, localization and single-organism process, extracellular region, extracellular region part and macromolecular complex, catalytic and binding activity (Fig. 4A). While totally 308 DEGs and 36 terms between two rearing densities after VPE1 challenge were enriched, mainly including metabolic, cellular and single-organism process, binding and catalytic activity, and organelle, cell and cell part (Fig. 4B). Also, some DEGs related stimulus and immunity were up-regulated, such as immune system process, response to stimulus, signal transducer activity, and virion and virion part. The KEGG analysis indicated that the top five enriched pathways of the DEGs in hepatopancreas between two rearing density were protein digestion and absorption, pancreatic secretion, neuroactive ligand-receptor interaction, glycine, serine and threonine metabolism, and protein processing in endoplasmic reticulum (Fig. 5A). After VPE1 challenge, most enriched pathways in the hepatopancreas between two rearing density fell into the categories of aminoacyl-tRNA biosynthesis, followed by fructose and mannose metabolism, biosynthesis of amino acids, folate biosynthesis, and glycolysis/gluconeogenesis (Fig. 5B).

Meanwhile, the results of GLM analysis showed that totally 20 DEGs were identified in the LH and HH group, with 9 and 11 genes up- and down-regulated, respectively. Exposure to the VPE1 led to differential expression of 928 genes in LHC and HHC group, corresponding to 824 and 104 genes up- and down-regulated, respectively (Fig. S7). GO enrichment analysis showed 15 DEGs and 5 terms were enriched between two rearing densities, involving in metabolic process, single-organism process, cellular process, catalytic and binding activity (Fig. S8A). While 432 DEGs and 36 terms between two rearing densities after VPE1 challenge were enriched, mainly involving in cellular, metabolic and single-organism process, binding and catalytic activity, and cell, cell part and organelle (Fig. S8B). Furthermore, the top five enriched pathways of the DEGs in hepatopancreas between two rearing density were lectins, biosynthesis of unsaturated fatty acids, cysteine and methionine metabolism, fatty acid metabolism and glycine, serine and threonine metabolism (Fig. S9A). After VPE1 challenge, most enriched pathways in the hepatopancreas between two rearing density fell into the categories of RNA transport, followed by aminoacyl-tRNA biosynthesis, spliceosome, carbon metabolism and biosynthesis of amino acids (Fig. 5B).

3.6. Comparative analysis of the L. vannamei intestinal transcriptomic response to VPE1 challenge between different rearing densities

To examine the transcriptomic effects of rearing density on *L. vannamei* intestinal response to VPE1 challenge, we compared gene expression between LI-HI and LIC-HIC groups, respectively. The results of negative binomial distribution difference analysis indicated that rearing density gave rise to differential expression of 5470 genes in the intestine, corresponding to 5206 and 264 genes up- and down-regulated, respectively. Then, exposure to the VPE1 resulted in differential expression of 279 genes in LIC and HIC group, corresponding to 132 and 147 genes up- and down-regulated, respectively (Fig. 3A). Totally 300 common DEGs were identified from LI-HI and LIC-HIC groups (Fig. 3C). As shown in Fig. 6A through GO functional enrichment analysis, a total of 2303 DEGs and 39 terms were enriched in intestine between two rearing density, mainly involving in metabolic, cellular, single-organism and biological regulation process, catalytic, binding and transporter activity, cell, cell part and organelle. Most DEGs related stimulus and immunity were also up-regulated, which was in accord with the results of hepatopancreas between two rearing density. After VPE1 challenge, totally 107 DEGs and 20 terms between two rearing densities were enriched through GO enrichment analysis, mainly referring to

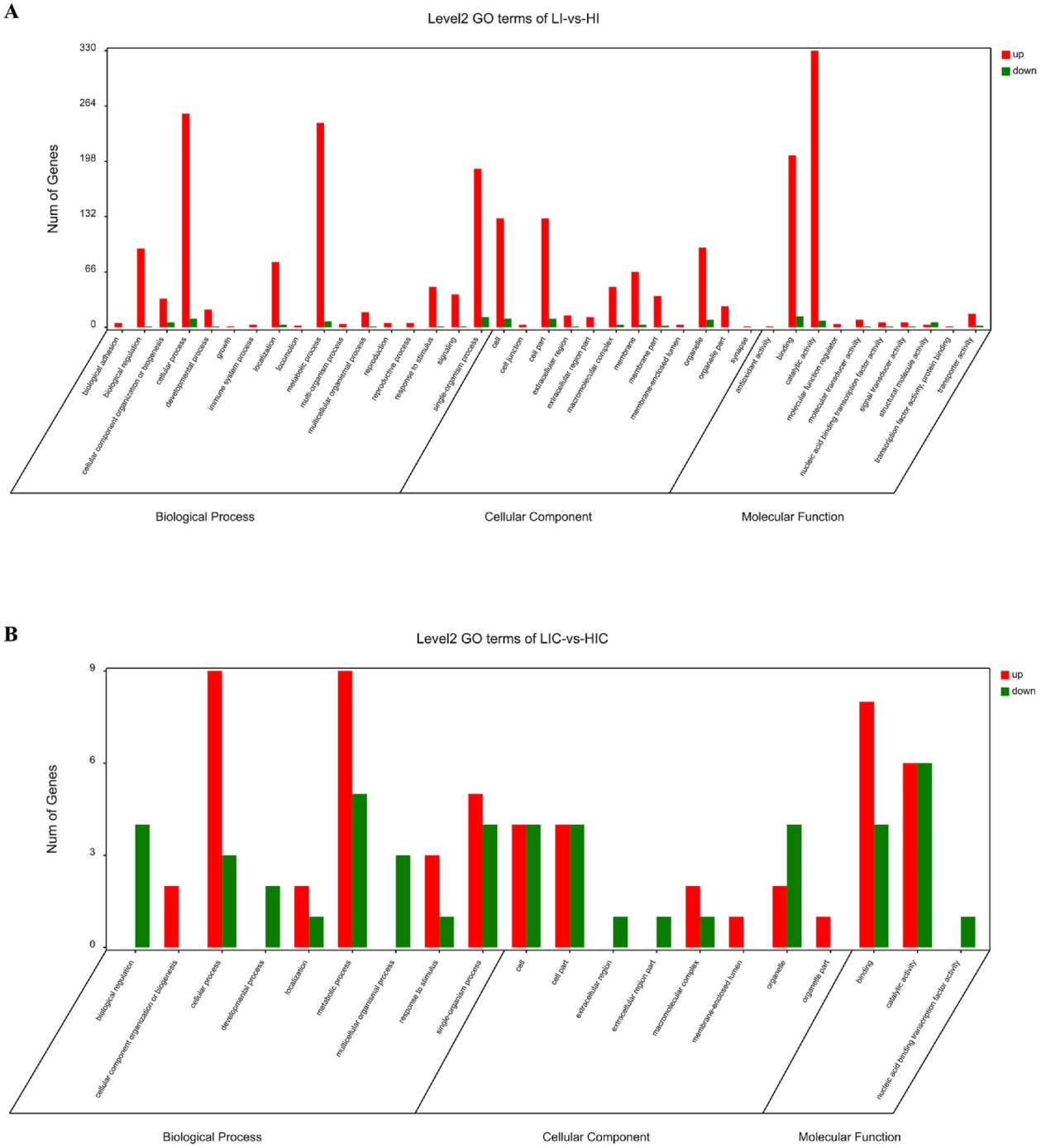

Fig. 6. A. GO enrichment analysis of DEGs in intestine of *L. vannamei* in LD-HD groups. **B.** GO enrichment analysis of DEGs in intestine of *L. vannamei* in LDC-HDC groups.

metabolic, cellular and single-organism process, binding and catalytic activity, cell, cell part and organelle (Fig. 6B). Through KEGG analysis, the most enriched five pathways of the DEGs in intestine between two rearing densities were membrane trafficking, mTOR signaling pathway, ubiquitin system, SNARE interactions in vesicular transport and endocytosis (Fig. 7A). While the most significantly regulated genes in the intestine between two rearing densities after VPE1 challenge were related to aminoacyl-tRNA biosynthesis, ECM-receptor interaction, ribosome biogenesis in eukaryotes, glycosphingolipid biosynthesis-ganglio series and ferroptosis (Fig. 7B).

The results of GLM analysis showed that rearing density resulted in 6509 DEGs in the intestine, corresponding to 6223 and 286 genes up- and down-regulated, respectively. A total of 202 DEGs were identified in intestine from the LIC and HIC group, with 71 and 131 genes up- and down-regulated, respectively (Fig. S7). GO functional enrichment analysis showed totally of 2775 DEGs and 43 terms were enriched in intestine between two rearing density, mainly involving in cellular, metabolic and single-organism process, catalytic and binding activity, cell, cell part and organelle (Fig. S10A). 92 DEGs and 19 terms between two rearing densities after VPE1 challenge were enriched, mainly involving in metabolic, cellular and single-organism process, binding and catalytic activity, and cell, cell part and organelle (Fig. S10B). KEGG analysis showed that the most enriched five pathways of the DEGs in intestine between two rearing densities were membrane trafficking,

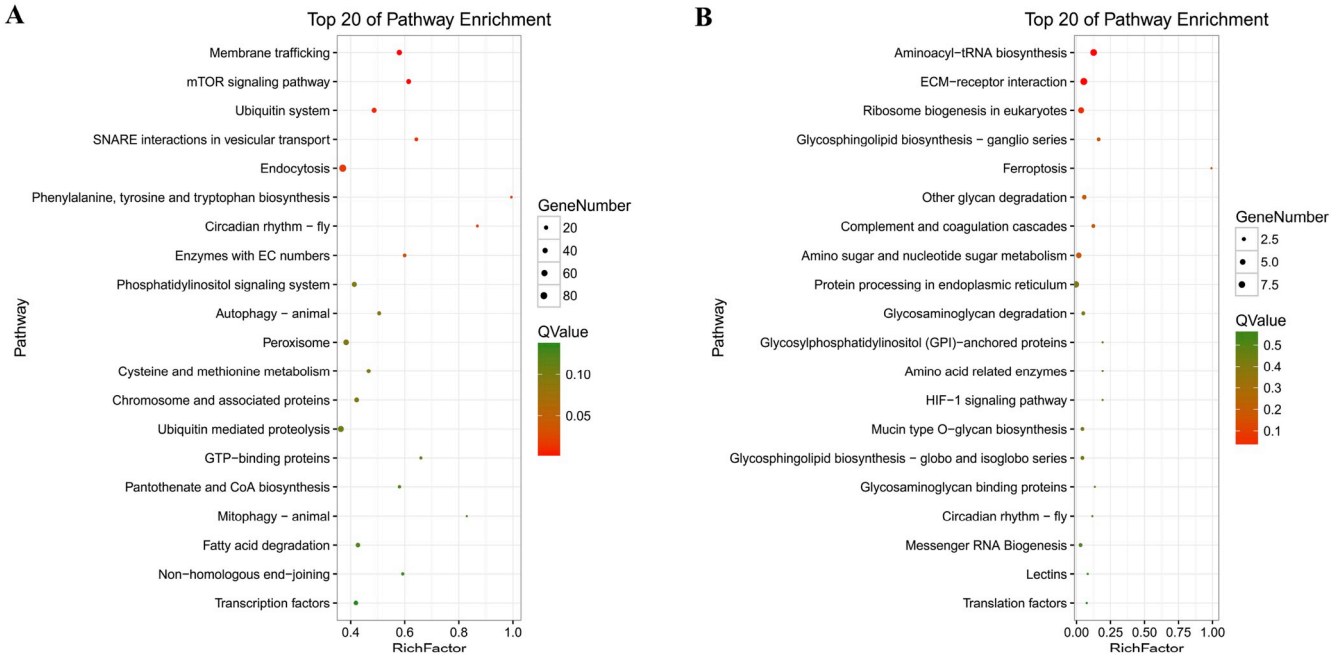

Fig. 7. A. Top 20 significantly enriched KEGG pathways of DEGs in intestine of *L. vannamei* in LD-HD groups. **B.** Top 20 significantly enriched KEGG pathways of DEGs in intestine of *L. vannamei* in LDC-HDC groups.

mTOR signaling pathway, peroxisome, SNARE interactions in vesicular transport and basal transcription factors (Fig. S11A). While the most significantly regulated genes in the intestine between two rearing densities after VPE1 challenge were related to aminoacyl-tRNA biosynthesis, ECM-receptor interaction, mucin type O-glycan biosynthesis, glycosphingolipid biosynthesis-keratan sulfate and amino sugar and nucleotide sugar metabolism (Fig. S11B).

3.7. Density-specific immune responses to VPE1 challenge

To understand the potential transcriptomic underpinnings for the differences in disease susceptibility between rearing densities, we identified DEGs and pathways related to immune system unique to each density and infected treatment through negative binomial distribution difference analysis. Based on the KEGG pathway annotations, the DEGs in hepatopancreas were grouped into only four pathways related to animal immune system under different densities, including lections, MAPK signaling pathway, endocytosis and phagosome (Table 2). However, most DEGs in hepatopancreas exhibited significantly up-regulated which involved into fourteen pathways related to immune response under different densities after VPE1-infected. In addition to the pathways mentioned above, they also include NOD-like receptor signaling pathway, Toll-like receptor signaling pathway, lysosome, proteasome, Jak-STAT signaling pathway, RIG-I-like receptor signaling pathway, and so on (Table 2). Potential regulatory relationship of DEGs with the highest person correlation coefficient in hepatopancreas selected for immune response to VPE1 challenge between different rearing densities was showed in Fig. 8A. Correlation analysis showed that all the DEGs were positively correlated. The DEGs (such as C7M84_000088, C7M84_000269) at the center of regulatory networks were mainly involving in JAK-STAT signaling pathway and lysosome.

In contrast, seventeen significantly changed pathways related to the immune system were found in the intestine under different densities, such as MAPK signaling pathway, ubiquitin mediated proteolysis, NOD-like receptor signaling pathway, endocytosis, autophagy, peroxisome, and so on (Table 3). Meanwhile, most of DEGs were exhibited obviously up-regulated. While the DEGs in intestine were mostly down-regulated and only grouped into five pathways associated with immune response under different densities after VPE1-infected. These pathways were lectins, lysosome, phagosome, ubiquitin mediated proteolysis and complement and coagulation cascades (Table 3). As showed in Fig. 8B, all DEGs with the highest person correlation coefficient in intestine selected for immune response to VPE1 challenge between different rearing densities were positively correlated. The DEGs (such as C7M84_000081, C7M84_000305, C7M84_000138) at the center of regulatory networks were mainly involving in lysosome, lectins and ubiquitin mediated proteolysis. Additionally, the similar results were showed through the method of GLM analysis (Table S3 and Table S4).

3.8. Verification of transcriptomic sequencing by qPCR

To confirm and refine the transcriptomic sequencing data, qPCR analysis of twenty randomly selected DEGs from hepatopancreas and intestine were performed, respectively. The results showed all tested genes from qPCR were concordant direction of change with the transcriptome sequencing data (Fig. S12).

4. Discussion

Rearing density and disease management are considered pivotal factors determining shrimp farm productivity and profitability [11,28]. HD, as one of the vital factors disrupts shrimp's homeostasis and affects their immunocompetence and disease susceptibility, inducing disease with a gradual decline of reared shrimp stock quality and profitability, thus causing a significant problem in aquaculture practices [18,23]. In the present study, HD exhibited a negative effect on growth performance and induced a significantly higher mortality than the low rearing shrimp, which indicated that there were substantial differences in susceptibility to VPE1 challenge between the two rearing densities. This study had also manifested the ability of HD to destroy the histopathology of shrimp including hepatic tubule, hepatocytes and intestinal epithelial cells, resulting in the breakdown of the hepatopancreas and intestine structure. Previous studies also proved that HD result in negative growth, survival, histopathology and the emergence of pathogen outbreaks [4,29,30]. Furthermore, compared to the LD shrimp, the HD shrimp showed more severe structural damage after

Table 2
Most DEGs in hepatopancreas selected for immune response to VPE1 infection between different stocking densities.

Gene ID	Annotation	log2(FC)	FDR
LD-VS-HD			
Lectins			
XLOC_026489	Predicted: hepatic lectin-like [*Hyalella azteca*]	−2.73	3.86E-03
MAPK signaling pathway			
C7M84_025108	heat shock protein [*Cherax destructor*]	−3.78	1.49E-02
Endocytosis			
C7M84_025108	heat shock protein [*Cherax destructor*]	−3.78	1.49E-02
Phagosome			
C7M84_011158	Predicted: protein transport protein Sec61 subunit alpha isoform 2-like [*Biomphalaria glabrata*]	−5.07	1.40E-02
LDC-VS-HDC			
Lectins			
XLOC_031461	fibrinogen-related protein isoform 1 [*Litopenaeus vannamei*]	3.12	1.10E-02
MAPK signaling pathway			
C7M84_011018	Predicted: torso-like protein [*Aethina tumida*]	−1.65	04.05E-02
C7M84_022853	mitogen-activated protein kinase [*Fenneropenaeus chinensis*]	1.46	3.98E-02
Endocytosis			
C7M84_008392	RhoA [*Marsupenaeus japonicus*]	−1.60	1.14E-02
C7M84_024376	Predicted: vascular endothelial growth factor receptor 2-like [*Neodiprion lecontei*]	2.09	2.89E-02
Phagosome			
C7M84_006247	Predicted: proclotting enzyme isoform X3 [*Trachymyrmex zeteki*]	8.51	2.17E-04
C7M84_011240	Predicted: tubulin alpha-3 chain-like [*Hyalella azteca*]	2.62	9.66E-04
C7M84_012998	integrin alpha 5 [Fenneropenaeus chinensis]	1.90	3.57E-02
C7M84_015801	integrin beta subunit [*Litopenaeus vannamei*]	1.89	9.27E-04
C7M84_018077	beta-II tubulin [*Homarus americanus*]	1.56	2.54E-02
C7M84_024387	Predicted: tubulin alpha-8 chain-like [*Hyalella azteca*]	2.59	1.2E-03
NOD-like receptor signaling pathway			
C7M84_012326	Predicted: protein NLRC5-like [*Acropora digitifera*]	1.88	5.88E-03
C7M84_020513	caspase 4 [*Litopenaeus vannamei*]	1.47	4.77E-02
Toll-like receptor signaling pathway			
C7M84_020513	caspase 4 [*Litopenaeus vannamei*]	1.47	4.77E-02
Lysosome			
C7M84_000269	triacylglycerol lipase [*Portunus trituberculatus*]	3.05	2.35E-02
C7M84_008143	ecdysteroid regulated-like protein [*Litopenaeus vannamei*]	3.42	2.44E-02
C7M84_008716	Predicted: protein Malvolio isoform X2 [*Tribolium castaneum*]	2.21	1.1E-02
C7M84_010693	Predicted: sialin-like [*Hyalella azteca*]	3.25	1.86E-02
C7M84_027395	Predicted: putative glucosylceramidase 3 [Hyalella azteca]	1.68	4.77E-02
C7M84_014451	ecdysteroid-regulated protein [*Litopenaeus vannamei*]	−2.03	2.89E-02
Proteasome			
C7M84_001761	Predicted: 26S proteasome non-ATPase regulatory subunit 2-like [*Hyalella azteca*]	1.20	4.79E-02
C7M84_017290	Predicted: proteasome subunit beta type-1-like [*Hyalella azteca*]	1.41	1.48E-02
C7M84_018719	Predicted: 26S proteasome non-ATPase regulatory subunit 13-like [*Hyalella azteca*]	1.28	3.24E-02
JAK-STAT signaling pathway			
C7M84_020269	Predicted: serine/threonine-protein kinase pim-3-like [*Limulus polyphemus*]	1.44	3.08E-02
C7M84_010747	SOCS [*Litopenaeus vannamei*]	1.80	5.85E-03
RIG-I-like receptor signaling pathway			
C7M84_020513	caspase 4 [*Litopenaeus vannamei*]	1.47	4.77E-02
Complement and coagulation cascades			
C7M84_020269	serine proteinase inhibitor B3 [*Penaeus monodon*]	2.68	2.53E-02
Apoptosis			
C7M84_020513	caspase 4 [*Litopenaeus vannamei*]	1.47	4.77E-02
Ubiquitin mediated proteolysis			
C7M84_001539	ubiquitin-activating enzyme E1 [*Penaeus monodon*]	1.32	4.3E-02
C7M84_007625	Predicted: anaphase-promoting complex subunit 1-like [*Lingula anatina*]	1.26	4.86E-02
C7M84_008997	DNA damage-binding protein 1 [*Eriocheir sinensis*]	1.20	4.77E-02
C7M84_011188	ubiquitin-conjugating enzyme E2 [*Fenneropenaeus chinensis*]	1.29	3.78E-02
C7M84_022477	Ubiquitin-conjugating enzyme/RWD-like protein [*Pseudocohnilembus persalinus*]	2.14	2.31E-02
Peroxisome			
C7M84_008996	Predicted: long chain acyl-CoA synthetase 9, chloroplastic-like [*Hyalella azteca*]	1.83	4.2E-03
C7M84_017167	Predicted: dihydroxyacetone phosphate acyltransferase-like isoform X2 [*Lingula anatina*]	1.75	4.64E-02

exposure to VPE1. Here we demonstrated that higher rearing levels significantly altered shrimp disease responses at the growth and histopathology level, and result in higher disease susceptibility.

Oxidative stress response is essential defense mechanism for crustaceans to resist invading microorganisms by producing large amounts of reactive oxygen species (ROS) [31,32]. Nevertheless, it will inevitably produce over-expression of ROS with the process of aerobic metabolism with the process of aerobic metabolism, resulting in oxidative damage to cells and tissues. Cells have developed a set of antioxidant defense systems involving many antioxidant enzymes, such as SOD, CAT, GPX, to protect themselves against oxidative stress and prevent oxidative damage [33]. The results of our study showed that the antioxidant enzymes activities of shrimp were significantly suppressed by density stress, and then resulting in poor antioxidant capacity response to VPE1 challenge. Lin et al. reported that *L. vananmei* reared at high densities (> 10 shrimp L^{-1}) exhibited decreased resistance against *V. alginolyticus* and white spot syndrome virus as evidenced by reductions in immune parameters (such as SOD, GSH-PX activities) [4].

For the transcriptional level, two different rearing densities led to 45 DEGs (29 up-regulated and 16 down-regulated) in hepatopancreas of shrimp. While, a total of 5470 DEGs (5206 up-regulated and 264 down-

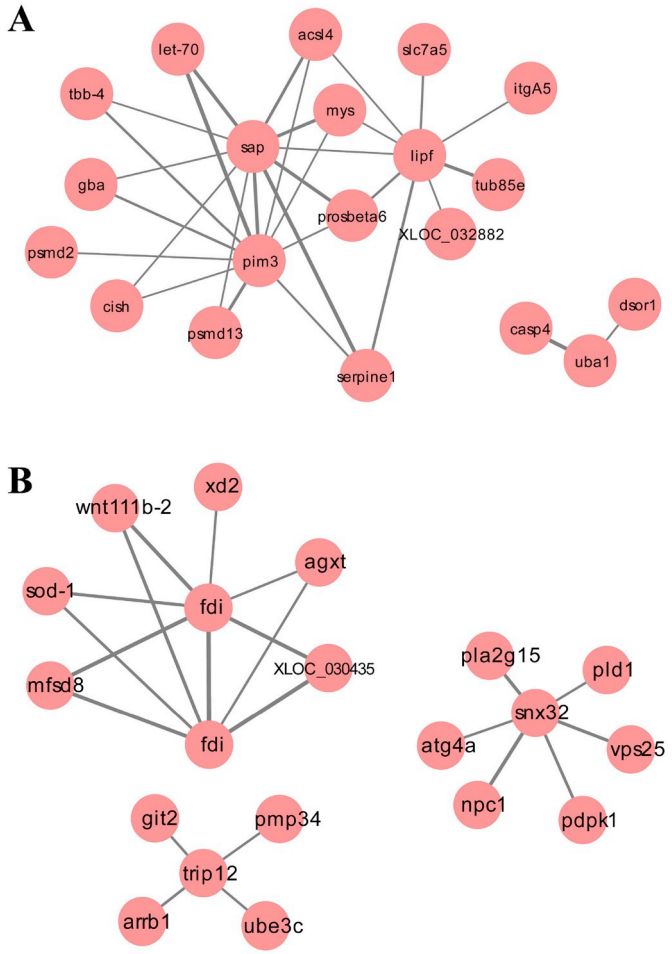

Fig. 8. A. Network view of top 20 DEGs with the highest correlation coefficient in hepatopancreas (A) and intestine (B) selected for immune response to VPE1 infection between different stocking densities. Edge line width represents connection strength (weight); Thicker lines denote stronger connections; Color lines represents positive and negative correlations; Gray lines represents positive correlations. (For interpretation of the references to color in this figure legend, the reader is referred to the Web version of this article.)

regulated) were identified in the intestine. Consistent with this, the number of enriched GO terms and KEGG pathways in the intestine of shrimp under two different densities were more than those of hepatopancreas. The above results suggested that density stress brought about impact in varying degrees on hepatopancreas and intestinal tract of shrimp, and here we preliminarily proposed that the intestinal of shrimp was more sensitive to density stress than hepatopancreas from the view of transcriptome level. On the contrary, previous studies proved the hepatopancreas of *L. vannamei* was more sensitive to other environmental factors (such as low dissolved oxygen (DO), pH and aflatoxin B1 (AFB1)) than the intestine [34–36], which suggested that the preference of the organ function in *L. vannamei* was also affected by the type of stimulus. After VPE1 challenge, we obtained 639 DEGs in hepatopancreas under two different rearing density, while 279 ones were identified in the intestine, which indicated early density stress resulted in differences in the response of hepatopancreas and intestine to VPE1 challenge in both density conditions.

Studies have demonstrated that the degree of damage caused by pathogen largely depends on the host immune system including humoral and cellular immune responses [37,38]. *L. vannamei*, as invertebrate, rely on only innate immunity to defense invading microbes [39]. Thus, we further analyzed the DEGs and pathways related immune system unique to each density and infected treatment to explore the potential influence mechanisms of rearing density on immune response to VPE1 challenge.

Lectins, as a specialized group of immune recognition molecules, play essential roles in immune recognition and phagocytosis through opsonization in crustaceans [40]. Toll-like receptors (TLRs) are kinds of single, membrane-spanning, non-catalytic receptors that recognize structurally conserved molecules of microbes and active immune cell responses [41]. The NOD-like receptors (NLRs), as a class of intracellular receptors, are also key components of the host innate immune system. Evidences have proved that NLRs could sense conserved microbial molecules to activate discrete signaling pathways including nuclear factor-kappa B (NF-κB) and mitogen-activated protein kinase (MAPK) pathways [42]. Furthermore, NLRs and TLRs could also cooperate to regulate the inflammatory response against microbes. In this study, the pathways related to immune recognition (such as lectins, Toll-like receptors and NOD-like receptors pathways) in hepatopancreas and intestinal of HD shrimp were significantly disordered, indicating that density stress had a certain effect on the process of hepatopancreas and intestine innate immune recognition, especially on intestine.

JAK/STAT and Immune deficiency (IMD) pathways are regarded as the main pathways regulating the humoral immune response of invertebrates to pathogen, while phagosome, endocytosis, apoptosis and autophagy are integral parts of cellular immunity [43,44]. In this study, density stress or VPE1-infected exhibited significant change in the pathways related to humoral and cellular immunity. Additionally, the innate immune response of animals to microbial infections is triggered by a variety of humoral and cellular immunity via signaling transduction pathways [45]. MAPK signaling pathway plays a key role in regulating inflammation and other diverse cellular functions, and is also involved in the immune response in shrimp [46]. AMP-activated protein kinase (AMPK) signaling pathway is another important signaling transduction pathway, which is regarded as a sensor of the cellular energy state, responding to metabolic stress [47]. In this study, MAPK signaling pathway was disordered in hepatopancreas after VPE1 challenge, while AMPK signaling pathway was maladjusted in intestine by density stress. Here we speculated the effects of pre-density stress on the immune system of shrimp involve various processes of immunity, including immune recognition, signal transduction and immune response, resulting in decreased ability to resist pathogen invasion and even death. Additionally, all above results indicated that hepatopancreas was regarded as the main immune of shrimp organ in response to the pathogen invasion, while intestine was mainly affected by environmental density stress.

5. Conclusion

To summarize, this study investigated the complex functional genomic effects of rearing density on shrimp immune responses and disease susceptibility. We demonstrated that high densities that likely induce increased social stress in shrimp result in altered immune responses to VPE1 challenge, decreased weight gain rate (63.20 ± 1.67% and 18.73 ± 3.35% in the HD and LD groups, respectively), severely destroyed the histopathology, inhibited the antioxidant enzymes activities, disordered the immune genes and pathways by the pathogen (such as Toll-like receptors, NOD-like receptors, JAK/STAT, IMD, MAPK and AMPK pathways), and thus higher mortality due to disease. We also proposed underlying differences in expression of genes between the two rearing densities significantly contribute to the observed variance in pathogen susceptibility. The results of this study not only provide a significant in-depth transcriptomic resource for future studies of rearing stress and immunity in shrimp, but offer a foundation for finding potential and feasible practical strategies for health management and disease prevention in shrimp aquaculture.

Table 3
Most DEGs in intestine selected for immune response to VPE1 infection between different stocking densities.

Gene ID	Annotation	log2(FC)	FDR
LD-VS-HD			
MAPK signaling pathway			
C7M84_017250	RAS [*Litopenaeus vannamei*]	2.23	6.86E-04
C7M84_022853	mitogen-activated protein kinase kinase [*Fenneropenaeus chinensis*]	2.01	5.74E-04
C7M84_024621	ERK [*Litopenaeus vannamei*]	1.90	8.4E-04
C7M84_024745	Predicted: ras GTPase-activating protein 3-like [*Hyalella azteca*]	1.69	3.20E-03
XLOC_027031	RAS [*Litopenaeus vannamei*]	1.70	2.54E-03
Ubiquitin mediated proteolysis			
C7M84_006509	Predicted: ubiquitin-conjugating enzyme E2 J1-like [*Limulus polyphemus*]	2.50	2.15E-05
C7M84_007144	Predicted: ubiquitin-conjugating enzyme E2 N [*Hyalella azteca*]	2.27	1.35E-04
C7M84_009996	ubiquitin-conjugating enzyme [*Litopenaeus vannamei*]	2.28	3.17E-05
C7M84_017463	Predicted: E3 ubiquitin-protein ligase HERC2-like [*Limulus polyphemus*]	1.87	3.16E-0
XLOC_018503	Predicted: E3 ubiquitin-protein ligase RFWD2-like [*Hyalella azteca*]	2.14	1.50E-4
C7M84_011166	Predicted: ubiquitin-protein ligase E3C [*Solenopsis invicta*]	1.42	5.76E-03
NOD-like receptor signaling pathway			
C7M84_017287	Predicted: uncharacterized protein [*Hyalella azteca*]	1.36	6.93E-03
C7M84_017818	Predicted: protein LAP2-like [*Limulus polyphemus*]	1.52	1.1E-03
C7M84_020513	caspase 4 [*Litopenaeus vannamei*]	1.44	1.08E-02
C7M84_020595	TGF-beta-activated kinase 1 and MAP3K7-binding protein 2 [*Litopenaeus vannamei*]	1.41	1.75E-02
XLOC_030648	hypothetical protein [*Daphnia pulex*]	1.77	4.11E-03
Endocytosis			
C7M84_003281	Predicted: vacuolar protein-sorting-associated protein 25-like [*Hyalella azteca*]	2.47	8.31E-06
C7M84_007837	G protein-coupled receptor kinase type 2 [*Homarus americanus*]	2.14	6.17E-06
C7M84_012906	WSSV receptor Rab7, partial [*Penaeus monodon*]	2.12	8.49E-06
C7M84_015196	Rab10 [*Macrobrachium rosenbergii*]	2.05	4.09E-06
C7M84_015761	Predicted: phospholipase D alpha 1-like isoform X1 [*Hyalella azteca*]	2.11	6.23E-06
C7M84_002626	Predicted: ARF GTPase-activating protein GIT2-like [*Limulus polyphemus*]	1.15	4.63E-02
C7M84_004168	Beta-arrestin-1 [*Zootermopsis nevadensis*]	1.70	1.62E-03
C7M84_000305	Sorting nexin-6, partial [*Stegodyphus mimosarum*]	4.86	5.57E-03
Autophagy			
C7M84_000555	autophagy protein 5, partial [*Callinectes sapidus*]	2.17	1.72E-04
C7M84_014661	cysteine protease ATG4A [*Coptotermes formosanus*]	2.18	1.05E-04
C7M84_015662	Predicted: ubiquitin-like modifier-activating enzyme ATG7 [*Branchiostoma belcheri*]	1.84	4.4E-04
C7M84_025533	Predicted: serine/threonine-protein kinase ULK3-like [*Hyalella azteca*]	2.36	8.99E-05
XLOC_018051	autophagy-related protein 8 [*Litopenaeus vannamei*]	1.94	1.04E-04
Peroxisome			
C7M84_011332	Predicted: peroxisomal carnitine O-octanoyltransferase-like [*Hyalella azteca*]	2.41	2.58E-06
C7M84_015576	Predicted: serine-pyruvate aminotransferase-like isoform X2 [*Lingula anatina*]	3.44	1.24E-10
C7M84_023456	NADP-specific isocitrate dehydrogenase [*Riptortus pedestris*]	2.50	3.11E-06
XLOC_013015	Peroxisomal biogenesis factor 3 [*Zootermopsis nevadensis*]	2.01	1.24E-04
C7M84_023700	Predicted: D-aspartate oxidase [*Musca domestica*]	1.63	5.77E-04
C7M84_006325	copper/zinc superoxide dismutase isoform 2 [*Marsupenaeus japonicus*]	4.30	8.17E-03
C7M84_015088	Predicted: xanthine dehydrogenase 2-like [Hyalella azteca]	3.20	2.33E-03
C7M84_023113	Peroxisomal membrane protein PMP34 [Zootermopsis nevadensis]	1.64	1.70E-02
JAK-STAT signaling pathway			
C7M84_001264	domeless [*Litopenaeus vannamei*]	1.81	2.89E-04
C7M84_010466	Predicted: suppressor of cytokine signaling 7-like [*Tetranychus urticae*]	1.51	1.02E-02
C7M84_010592	phosphatidylinositol-4,5-bisphosphate 3-kinase catalytic subunit delta isoform [*Fenneropenaeus chinensis*]	1.55	1.94E-03
C7M84_010780	serine/threonine-specific protein kinase AKT [*Fenneropenaeus chinensis*]	1.85	4.04E-03
C7M84_023236	STAT [*Litopenaeus vannamei*]	1.44	3.37E-03
AMPK signaling pathway			
C7M84_001589	Ras-related protein Rab-8A [*Daphnia magna*]	2.32	4.21E-04
C7M84_016897	transforming growth factor beta-activated kinase 1 [*Litopenaeus vannamei*]	1.17	4.44E-02
Toll-like receptor signaling pathway			
C7M84_016897	transforming growth factor beta-activated kinase 1 [*Litopenaeus vannamei*]	1.17	4.44E-02
C7M84_020513	caspase 4 [*Litopenaeus vannamei*]	1.44	1.08E-02
Chemokine signaling pathway			
C7M84_021573	Predicted: neural Wiskott-Aldrich syndrome protein-like [*Hyalella azteca*]	1.85	2.39E-02
Lysosome			
C7M84_000080	Chitooligosaccharidolytic beta-N-acetylglucosaminidase [*Orchesella cincta*]	14.61	3.53E-10
C7M84_000081	Chitooligosaccharidolytic beta-N-acetylglucosaminidase [*Orchesella cincta*]	8.40	1.28E-06
C7M84_000497	Predicted: group XV phospholipase A2-like [*Limulus polyphemus*]	2.45	5.88E-06
C7M84_000860	Predicted: beta-mannosidase-like [*Hyalella azteca*]	1.88	2.85E-04
C7M84_009478	beta-N-acetylglucosaminidase [*Fenneropenaeus chinensis*]	9.91	5.94E-05
C7M84_014844	Predicted: major facilitator superfamily domain-containing protein 8-like [Hyalella azteca]	9.09	3.76E-02
C7M84_020508	Predicted: Niemann-Pick C1 protein-like isoform X1 [Hyalella azteca]	1.49	9.73E-03
RIG-I-like receptor signaling pathway			
C7M84_016897	transforming growth factor beta-activated kinase 1 [*Litopenaeus vannamei*]	1.17	4.44E-02
C7M84_020513	caspase 4 [*Litopenaeus vannamei*]	1.44	1.08E-02
TNF signaling pathway			
C7M84_016897	transforming growth factor beta-activated kinase 1 [*Litopenaeus vannamei*]	1.17	4.44E-02
Toll and Imd signaling pathway			
XLOC_017670	transforming growth factor beta-activated kinase 1 [*Litopenaeus vannamei*]	1.09	3.52E-02

(*continued on next page*)

Table 3 (*continued*)

Gene ID	Annotation	log2(FC)	FDR
Apoptosis			
C7M84_020513	caspase 4 [*Litopenaeus vannamei*]	1.44	1.08E-02
C7M84_021250	apoptosis-inducing factor [*Litopenaeus vannamei*]	1.20	1.40E-02
C7M84_024262	Predicted: DNA fragmentation factor subunit beta-like [*Saccoglossus kowalevskii*]	2.08	4.75E-03
XLOC_027031	RAS [*Litopenaeus vannamei*]	1.70	2.54E-03
XLOC_031171	Predicted: caspase-2 [*Pseudopodoces humilis*]	1.59	3.32E-02
Phagosome			
C7M84_001970	thrombospondin [*Fenneropenaeus merguiensis*]	14.43	3.58E-05
C7M84_002434	thrombospondin [*Fenneropenaeus merguiensis*]	14.62	2.70E-05
C7M84_003679	calnexin [*Penaeus monodon*]	2.30	5.52E-05
C7M84_006291	C-type lectin-like domain-containing protein PtLP [*Portunus trituberculatus*]	3.83	6.49E-07
C7M84_020064	Predicted: vesicle-trafficking protein SEC22b-B [*Fopius arisanus*]	2.28	9.07E-05
Leukocyte transendothelial migration			
C7M84_003046	actin 1 [*Fenneropenaeus chinensis*]	−7.00	5.12E-03
C7M84_012606	actin 2 [*Penaeus monodon*]	−11.43	8.78E-03
C7M84_015874	actin 2 [*Penaeus monodon*]	−12.39	1.00E-02
LDC-VS-HDC			
Lectins			
XLOC_007369	hypothetical protein [*Branchiostoma floridae*]	−2.58	1.69E-02
Lysosome			
C7M84_000081	Chitooligosaccharidolytic beta-N-acetylglucosaminidase [*Orchesella cincta*]	−9.64	1.71E-02
C7M84_009852	beta-N-acetylglucosaminidase [*Litopenaeus vannamei*]	−2.24	4.28E-02
C7M84_011026	saposin isoform 1 [*Penaeus monodon*]	2.91	3.17E-02
C7M84_022638	Predicted: sialin-like [*Hyalella azteca*]	5.91	1.32E-02
Phagosome			
C7M84_002358	perlucin 5 [*Haliotis diversicolor*]	−11.45	1.80E-03
C7M84_019241	tubulin beta, partial [*Litopenaeus vannamei*]	−1.45	8.78E-03
Ubiquitin mediated proteolysis			
C7M84_016948	Predicted: SUMO-activating enzyme subunit 2-like [*Branchiostoma belcheri*]	3.74	1.02E-03
Complement and coagulation cascades			
C7M84_020269	serine proteinase inhibitor B3 [*Penaeus monodon*]	1.34	3.03E-02
C7M84_024462	Predicted: complement factor H-related protein 4-like [*Hyalella azteca*]	−8.42	2.37E-02

Acknowledgements

The authors are grateful to all the laboratory members for their technical advice and helpful discussion. This study was financially supported by the Marine S&T Fund of Shandong Province for Pilot National Laboratory for Marine Science and Technology (Qingdao) (2018SDKJ0502-2), and the Science and Technology Development Fund Project of Shinan district, Qingdao city, China (2018-4-001-ZH).

Appendix A. Supplementary data

Supplementary data to this article can be found online at https://doi.org/10.1016/j.fsi.2019.08.004.

References

[1] F. yearbook, Fishery and Aquaculture Statistics 2016, (2018) Rome/Roma.
[2] G. Cuzon, A. Lawrence, G. Gaxiola, C. Rosas, J. Guillaume, Nutrition of *Litopenaeus vannamei* reared in tanks or in ponds, Aquaculture 235 (1) (2004) 513–551.
[3] J. Wilson Wasielesky, C. Froes, G. Fóes, D. Krummenauer, G. Lara, L. Poersch, Nursery of *Litopenaeus vannamei* reared in a biofloc system: the effect of stocking densities and compensatory growth, J. Shellfish Res. 32 (3) (2013) 799–806.
[4] Y.C. Lin, J.C. Chen, Y.Y. Chen, S.T. Yeh, L.L. Chen, C.L. Huang, J.F. Hsieh, C.C. Li, Crowding of white shrimp *Litopenaeus vananmei* depresses their immunity to and resistance against *Vibrio alginolyticus* and white spot syndrome virus, Fish Shellfish Immunol. 45 (1) (2015) 104–111.
[5] J.P. Apun-Molina, A. Robles-Romo, P. Alvarez-Ruiz, A. Santamaria-Miranda, O. Arjona, I.S. Racotta, Influence of stocking density and exposure to white spot syndrome virus in biological performance, metabolic, immune, and bioenergetics response of whiteleg shrimp *Litopenaeus vannamei*, Aquaculture 479 (2017) 528–537.
[6] S. Xia, Y. Li, W. Wang, M. Rajkumar, K.P.K. Vasagam, H. Wang, Influence of dietary protein levels on growth, digestibility, digestive enzyme activity and stress tolerance in white-leg shrimp, *Litopenaeus vannamei* (Boone, 1931), reared in high-density tank trials, Aquacult. Res. 41 (12) (2010) 1845–1854.
[7] Y. Li, J. Li, Q. Wang, The effects of dissolved oxygen concentration and stocking density on growth and non-specific immunity factors in Chinese shrimp, *Fenneropenaeus chinensis*, Aquaculture 256 (1–4) (2006) 608–616.
[8] S.J. Arnold, F.E. Coman, C.J. Jackson, S.A. Groves, High-intensity, zero water-exchange production of juvenile tiger shrimp, *Penaeus monodon*: an evaluation of artificial substrates and stocking density, Aquaculture 293 (1–2) (2009) 42–48.
[9] R. Calado, J. Figueiredo, R. Rosa, M.L. Nunes, L. Narciso, Effects of temperature, density, and diet on development, survival, settlement synchronism, and fatty acid profile of the ornamental shrimp *Lysmata seticaudata*, Aquaculture 245 (1–4) (2005) 221–237.
[10] J. Palma, D.P. Bureau, M. Correia, J.P. Andrade, Effects of temperature, density and early weaning on the survival and growth of Atlantic ditch shrimp *Palaemonetes varians* larvae, Aquacult. Res. 40 (13) (2009) 1468–1473.
[11] S.J. Arnold, M.J. Sellars, P.J. Crocos, G.J. Coman, An evaluation of stocking density on the intensive production of juvenile brown tiger shrimp (*Penaeus esculentus*), Aquaculture 256 (1–4) (2006) 174–179.
[12] D.V. Lightner, The penaeid shrimp viruses TSV, IHHNV, WSSV, and YHV, J. Appl. Aquac. 9 (2) (1999) 27–52.
[13] S.A. Soto Rodriguez, B. Gomez Gil, R. Lozano, A. Roque, Density of *vibrios* in hemolymph and hepatopancreas of diseased pacific white shrimp, *Litopenaeus vannamei*, from northwestern Mexico, J. World Aquac. Soc. 41 (2010) 76–83.
[14] P. Van West, *Saprolegnia parasitica*, an oomycete pathogen with a fishy appetite: new challenges for an old problem, Mycologist 20 (3) (2006) 99–104.
[15] T. Ellis, B. North, A. Scott, N. Bromage, M. Porter, D. Gadd, The relationships between stocking density and welfare in farmed rainbow trout, J. Fish Biol. 61 (3) (2002) 493–531.
[16] S. Thitamadee, A. Prachumwat, J. Srisala, P. Jaroenlak, P.V. Salachan, K. Sritunyalucksana, T.W. Flegel, O. Itsathitphaisarn, Review of current disease threats for cultivated penaeid shrimp in Asia, Aquaculture 452 (2016) 69–87.
[17] M. Zorriehzahra, R. Banaederakhshan, Early mortality syndrome (EMS) as new emerging threat in shrimp industry, Adv. Anim. Vet. Sci. 3 (2S) (2015) 64–72.
[18] G. Liu, S. Zhu, D. Liu, X. Guo, Z. Ye, Effects of stocking density of the white shrimp *Litopenaeus vannamei* (Boone) on immunities, antioxidant status, and resistance against *Vibrio harveyi* in a biofloc system, Fish Shellfish Immunol. 67 (2017) 19–26.
[19] R.P. Ellis, H. Parry, J.I. Spicer, T.H. Hutchinson, R.K. Pipe, S. Widdicombe, Immunological function in marine invertebrates: responses to environmental perturbation, Fish Shellfish Immunol. 30 (6) (2011) 1209–1222.
[20] J.H.W.M. Rombout, L. Abelli, S. Picchietti, G. Scapigliati, V. Kiron, Teleost intestinal immunology, Fish Shellfish Immunol. 31 (5) (2011) 616–626.
[21] C. Qi, L. Wang, M. Liu, K. Jiang, M. Wang, W. Zhao, B. Wang, Transcriptomic and morphological analyses of *Litopenaeus vannamei* intestinal barrier in response to *Vibrio paraheamolyticus* infection reveals immune response signatures and structural disruption, Fish Shellfish Immunol. 70 (2017) 437–450.
[22] V. Aguilar, I.S. Racotta, E. Goytortua, M. Wille, P. Sorgeloos, R. Civera, E. Palacios, The influence of dietary arachidonic acid on the immune response and performance of Pacific whiteleg shrimp, *Litopenaeus vannamei*, at high stocking density, Aquacult. Nutr. 18 (3) (2012) 258–271.
[23] Y. Gao, Z. He, H. Vector, B. Zhao, Z. Li, J. He, J.-Y. Lee, Z. Chu, Effect of stocking

density on growth, oxidative stress and HSP 70 of pacific white shrimp *Litopenaeus vannamei*, Turk. J. Fish. Aquat. Sci. 17 (5) (2017) 877–884.
[24] B. Langmead, S.L. Salzberg, Fast gapped-read alignment with Bowtie 2, Nat. Methods 9 (4) (2012) 357-U54.
[25] D. Kim, G. Pertea, C. Trapnell, H. Pimentel, R. Kelley, S.L. Salzberg, TopHat2: accurate alignment of transcriptomes in the presence of insertions, deletions and gene fusions, Genome Biol. 14 (4) (2013) R36-R36.
[26] B. Li, C.N. Dewey, RSEM: accurate transcript quantification from RNA-Seq data with or without a reference genome, BMC Bioinf. 12 (2011).
[27] K.J. Livak, T.D. Schmittgen, Analysis of relative gene expression data using real-time quantitative PCR and the 2(T)(-Delta Delta C) method, Methods 25 (4) (2001) 402–408.
[28] J.M.J. Ruiz-Velazco, A. Hernandez-Llamas, V.M. Gomez-Munoz, Management of stocking density, pond size, starting time of aeration, and duration of cultivation for intensive commercial production of shrimp *Litopenaeus vannamei*, Aquacult. Eng. 43 (3) (2010) 114–119.
[29] G.L. Allan, G.B. Maguire, Effects of stocking density on production of *Penaeus monodon* Fabricius in model farming ponds, Aquaculture 107 (1) (1992) 49–66.
[30] S.J. Arnold, F.E. Coman, C.J. Jackson, S.A. Groves, High-Intensity, zero water-exchange production of juvenile tiger shrimp, *Penaeus monodon*: an evaluation of artificial substrates and stocking density, Aquaculture 293 (1) (2009) 42–48.
[31] U. Bandyopadhyay, D. Das, R.K. Banerjee, Reactive oxygen species: oxidative damage and pathogenesis, Curr. Sci. 77 (5) (1999) 658–666.
[32] Y. Duan, J. Zhang, H. Dong, Y. Wang, Q. Liu, H. Li, Oxidative stress response of the black tiger shrimp *Penaeus monodon* to *Vibrio parahaemolyticus* challenge, Fish Shellfish Immunol. 46 (2) (2015) 354–365.
[33] W.N. Wang, J. Zhou, P. Wang, T.T. Tian, Y. Zheng, Y. Liu, W.J. Mai, A.L. Wang, Oxidative stress, DNA damage and antioxidant enzyme gene expression in the Pacific white shrimp, *Litopenaeus vannamei* when exposed to acute pH stress, Comp. Biochem. Physiol. C 150 (4) (2009) 428–435.
[34] S.Y. Han, M.Q. Wang, M. Liu, B.J. Wang, K.Y. Jiang, L. Wang, Comparative sensitivity of the hepatopancreas and midgut in the white shrimp *Litopenaeus vannamei* to oxidative stress under cyclic serious/medium hypoxia, Aquaculture 490 (2018) 44–52.
[35] S.Y. Han, M.Q. Wang, B.J. Wang, M. Liu, K.Y. Jiang, L. Wang, A comparative study on oxidative stress response in the hepatopancreas and midgut of the white shrimp *Litopenaeus vannamei* under gradual changes to low or high pH environment, Fish Shellfish Immunol. 76 (2018) 27–34.
[36] Y. Wang, B. Wang, M. Liu, K. Jiang, M. Wang, L. Wang, Comparative transcriptome analysis reveals the different roles between hepatopancreas and intestine of *Litopenaeus vannamei* in immune response to aflatoxin B1 (AFB1) challenge, Comp. Biochem. Physiol. C 222 (2019) 1–10.
[37] A. Tassanakajon, V. Rimphanitchayakit, S. Visetnan, P. Amparyup, K. Somboonwiwat, W. Charoensapsri, S. Tang, Shrimp humoral responses against pathogens: antimicrobial peptides and melanization, Dev. Comp. Immunol. 80 (2018) 81–93.
[38] S.Y. Lee, K. Soderhall, Early events in crustacean innate immunity, Fish Shellfish Immunol. 12 (5) (2002) 421–437.
[39] D. Hultmark, *Drosophila* immunity: paths and patterns, Curr. Opin. Immunol. 15 (1) (2003) 12–19.
[40] M. Marques, M.A. Barracco, Lectins, as non-self-recognition factors, in crustaceans, Aquaculture 191 (1) (2000) 23–44.
[41] Y. Kumagai, O. Takeuchi, S. Akira, Pathogen recognition by innate receptors, J. Infect. Chemother. 14 (2) (2008) 86–92.
[42] G. Chen, M.H. Shaw, Y.G. Kim, G. Nuñez, NOD-like receptors: role in innate immunity and inflammatory disease, Annu. Rev. Pathol. 4 (4) (2008) 365–398.
[43] J. Xiang, F. Li, Recent advances in researches on the innate immunity of penaeid shrimp, Fish Shellfish Immunol. 34 (6) (2013) 1685-1685.
[44] F. Li, J. Xiang, Recent advances in researches on the innate immunity of shrimp in China, Dev. Comp. Immunol. 39 (1–2) (2013) 11–26.
[45] N. Borregaard, P. Elsbach, T. Ganz, P. Garred, A. Svejgaard, Innate immunity: from plants to humans, Immunol. Today 21 (2) (2000) 68–70.
[46] L. Yang, X. Liu, J. Huang, Q. Yang, L. Qiu, W. Liu, S. Jiang, Molecular characterization and expression profile of MAP2K1ip1/MP1 gene from tiger shrimp, *Penaeus monodon*, Mol. Biol. Rep. 39 (5) (2012) 5811–5818.
[47] M. Hiroyuki, B.J. Goldstein, I. Motoyuki, A. Eiichi, AMPK and cell proliferation-AMPK as a therapeutic target for atherosclerosis and cancer, J. Physiol. 574 (1) (2010) 63–71.